

Impact of different initial soil moisture fields on Eta model weather forecasts for South America

L. Gustavo Goncalves de Goncalves,^{1,2} William James Shuttleworth,¹ Sin Chan Chou,³ Yongkang Xue,⁴ Paul R. Houser,⁵ David L. Toll,⁶ José Marengo,³ and Matthew Rodell⁶

Received 1 June 2005; revised 5 January 2006; accepted 8 May 2006; published 2 September 2006.

[1] Two 7-day weather simulations were made for South America in July 2003 and January 2004 (in the Southern Hemisphere summer and winter) to investigate the impacts of using different soil moisture initialization fields in the Eta model coupled to the Simplified Simple Biosphere (SSiB) land surface model. The alternative initial soil moisture fields were (1) the soil moisture climatology used operationally by the Centro de Previsão do Tempo e Estudos Climáticos in Brazil and (2) the soil moisture fields generated by a South American Land Data Assimilation System (SALDAS) based on SSiB. When the SALDAS soil moisture fields were used, there was an increase in the model performance relative to climatology in the equitable threat score calculated with respect to observed surface precipitation fields and a decrease (up to 53%) in the root-mean-square error relative to the NCEP analysis of the modeled geopotential height at 500 hPa and mean sea level pressure. However, there was small change in the model skill in positioning the primary South American weather systems because of a change in the upper troposphere circulation caused by SALDAS initialization, most noticeably in the South Atlantic Convergence Zone.

Citation: de Goncalves, L. G. G., W. J. Shuttleworth, S. C. Chou, Y. Xue, P. R. Houser, D. L. Toll, J. Marengo, and M. Rodell (2006), Impact of different initial soil moisture fields on Eta model weather forecasts for South America, *J. Geophys. Res.*, *111*, D17102, doi:10.1029/2005JD006309.

1. Introduction

[2] Soil moisture significantly impacts climate and weather simulations in numerical models by affecting the partitioning of energy between latent and sensible heat due to differences in the availability of heat and water at the surface. In this way, the initial soil moisture prescribed in a model can affect not only the near-surface air temperature and humidity, but also local atmospheric circulations and precipitation.

[3] Several studies have investigated the sensitivity of atmospheric models to soil moisture changes at different timescales in both seasonal and short-term simulations. *Shukla and Mintz* [1982] showed that simulated precipitation increases when using a wet initialization rather than dry initiation of land surfaces. By running a general circulation model (GCM) for several thousands of years,

Koster et al. [2000] concluded that predictions of precipitation are most influenced by soil moisture in the transition zones between humid and dry climates. *Fennessy and Shukla* [2000] and, more recently, *Zhang and Frederiksen* [2003] suggested that including observed soil moisture data in the initial conditions used in a model improves seasonal forecasts. At reduced temporal and spatial scales, it has been shown that the initiation of moist convection can be influenced by the spatial distribution of soil moisture [*Pielke*, 2001; *Weaver and Avissar*, 2001; *Findell and Eltahir*, 2003a, 2003b]. *Kanamitsu et al.* [2000] investigated the predictability of soil moisture and temperature in the NCEP seasonal forecast system using climatological and NCEP-DOE reanalysis 2 and found improved model skill over arid and semiarid regions where initial soil moisture conditions are critical.

[4] There has been considerable progress in the methodology of soil moisture data assimilation [*Houser et al.*, 1998; *Walker and Houser*, 2001; *Margulis et al.*, 2002; *Reichle et al.*, 2002; *Reichle and Koster*, 2003; *Crow and Wood*, 2003; *Seuffert et al.*, 2003], although the lack of observations in regions such as South America still compromises numerical simulations. Consequently, in South America the use of a Land Data Assimilation System [*Rodell et al.*, 2004] represents a promising alternative for ingesting ground-based and satellite observational data products by using land surface modeling and data assimilation techniques to generate optimal fields of land surface states and fluxes and initial fields of soil moisture.

¹Department of Hydrology and Water Resources, University of Arizona, Tucson, Arizona, USA.

²Now at Hydrological Sciences Branch, Code 614.3, NASA Goddard Space Flight Center, Greenbelt, Maryland, USA.

³Centro de Previsão do Tempo e Estudos Climáticos, Instituto Nacional de Pesquisas Espaciais, Cachoeira Paulista, Sao Paulo, Brazil.

⁴Department of Geography, University of California, Los Angeles, California, USA.

⁵Center for Research on Environment and Water, George Mason University, Calverton, Maryland, USA.

⁶Hydrological Sciences Branch, Code 614.3, NASA Goddard Space Flight Center, Greenbelt, Maryland, USA.

[5] Over the past few years, there has been an increasing effort to use regional models to better represent mesoscale processes, topography, coastal geometry, and land surface characteristics in South America, although several aspects of regional climate modeling such as resolution, lateral boundary conditions, initialization, spin-up time, and model variability remain poorly assessed [Giorgi and Mearns, 1999; Weisse *et al.*, 2000; Tanajura, 1996]. Tanajura and Shukla [2000] investigated the influence of the Andes on South American summer climate using the Eta model reinitialized every 48 hours. Chou *et al.* [2000] also used the Eta model over South America to make a detailed investigation of forecasts made with the Centro de Previsão de Tempo e Estudos Climáticos/Center for Ocean-Land-Atmosphere Studies (CPTEC/COLA) GCM [Bonatti, 1996] during opposite phases of the annual precipitation cycle. Seluchi *et al.* [2003] used the Eta model to study the extremely dry warm wind that occurs east of the Andes Cordillera (called the Zonda) that has an orographic origin similar to that of the Foehn that blows in Germany and Austria and the Chinook that occurs east of the Rocky Mountains. Chou *et al.* [2002] made a validation study of the Eta model coupled with a simplified version of Sellers *et al.*'s [1986] Simplified Simple Biosphere model (SSiB) [Xue *et al.*, 1991] over South America by performing 1 month simulations in the dry and wet seasons. This model is hereafter referred to as the "Eta-SSiB model."

[6] The present work investigates the impacts of soil moisture initialization in the Eta-SSiB model operating over South America with 40 km spatial resolution. The model is initialized using two different soil conditions. One is the soil moisture climatology used operationally at CPTEC, the resulting runs being here referred to as the control runs (CTR runs). The second used a product derived from a 3 year South American LDAS run made with an offline version of SSiB forced by the Global Data Assimilation System (GDAS) atmospheric fields for South America, the resulting being here referred to as SALDAS runs. Two 7 day runs were performed during the austral winter (in the dry season, in July 2003) and summer (in the wet season, in January 2004) using these different initial soil moisture conditions. The resulting 72 hours forecasts were then compared with each other and with observations. The models used are described in sections 2 and 3 and the soil moisture initialization procedures in section 4. Methods and analysis are explained in section 5 and results presented in section 6. Section 7 gives a summary and the conclusions.

2. Eta Model

[7] The Eta model is currently used as the primary regional model at CPTEC and is widely used at several other research and weather forecast centers worldwide. The version used at CPTEC was originally derived from that used at the National Centers for Environmental Prediction (NCEP) and calculates prognostic variables (i.e., temperature, specific humidity, horizontal wind components, surface pressure, turbulent kinetic energy and cloud water) on a 40 km semistaggered Arakawa E grid [Arakawa and Lamb, 1977] that covers most of South America and adjacent oceans.

[8] The Eta Model has the characteristic that it represents mountains as steps [Bryan, 1969] and it preserves all important conserved properties in its finite difference schemes [Mesinger *et al.*, 1988]. An improved Betts–Miller–Janjic scheme (BMJ) [Betts, 1986; Betts and Miller, 1986; Janjic, 1994] is employed to represent deep and shallow convection. The formulation of the large-scale condensation is conventional in this version of the Eta model, and includes the evaporation of precipitation in unsaturated layers below the condensation level [Janjic, 1990]. In the present study, the model was specified to have 28 levels, with the top of the atmosphere at 50 hPa. The vertical resolution is higher near the ground and near the tropopause. In the model runs, initial and lateral boundary conditions were taken from NCEP/GCM analyses in the form of spectral coefficients with T62 triangular truncation (equivalent to 1.825° resolution) in both the meridional and zonal directions. The 28 vertical layers were updated every 6 hours. Observed weekly average sea surface temperatures were used. The initial land surface albedo was also taken from the seasonal climatology routinely used at CPTEC, with subsequent values then calculated by SSiB.

3. SSiB Land Surface Scheme

[9] The Simplified Simple Biosphere land surface scheme (SSiB) [Xue *et al.*, 1991] used in the CPTEC Eta model is a simplified version of the Simple Biosphere model (SiB) [Sellers *et al.*, 1986]. It simulates biophysical processes by modeling vegetation explicitly. The SSiB scheme has three soil layers and one canopy layer, with eight prognostic variables (i.e., soil wetness in three soil layers; the temperatures of the canopy, ground surface, and deep soil layers; and the liquid water stored on the canopy and snow stored on the ground). The SSiB forcing variables (taken from the lowest modeled level of the Eta model) are precipitation, downward short-wave radiation, downward long-wave radiation, temperature, humidity, and wind speed. The output variables are surface albedo, the sensible heat flux, latent heat flux (transpiration and evaporation from intercepted water and the soil), momentum flux, ground heat fluxes, skin temperature, surface runoff, groundwater runoff, carbon dioxide flux, and net photosynthesis rate. SSiB requires the specification of 23 parameters for 13 ecosystems (i.e., broadleaf-evergreen, broadleaf deciduous trees, mixed forest, needleleaf evergreen trees, needleleaf deciduous trees, savanna, perennial grassland, broadleaf shrubs with ground cover, broadleaf shrubs with bare soil, tundra, desert, crops, and permanent ice). In the present study, the default values of the 23 parameters given by Xue *et al.* [1991] for each ecosystem were used. A recent study has been conducted to improve the snow parameterization in SSiB [Sun and Xue, 2001; Xue *et al.*, 2003] but this aspect of the model is not used in this study.

4. Eta/SSiB and Its Surface Initialization at CPTEC

[10] The present study uses the Eta model coupled to SSiB (Eta/SSiB model). The coupling methodology is described in detail by Xue *et al.* [2001], which study also reports that Eta/SSiB produces more realistic monthly

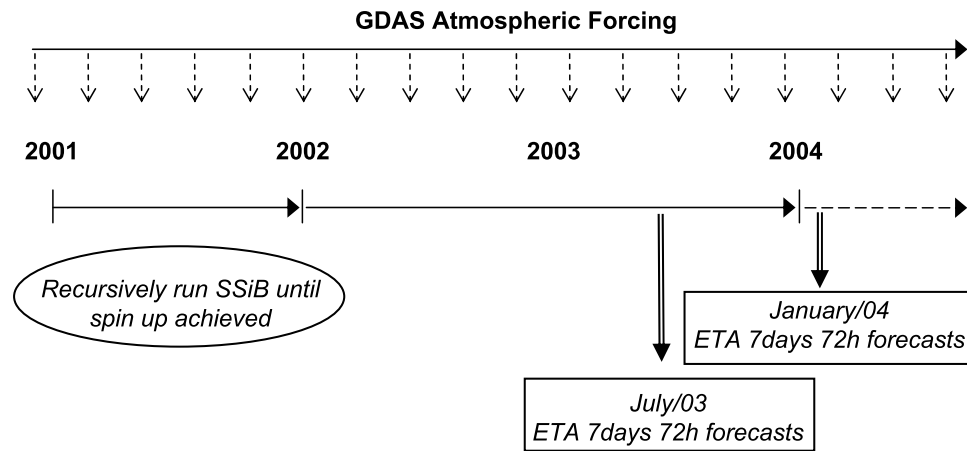


Figure 1. Diagram of the experiment design for the study showing how the initial SALDAS fields were generated for the two 72 hour Eta-SSiB runs during July 2003 and January 2004.

precipitation over United States than does the Eta model with a “bucket model” land surface scheme. The Eta/SSiB model evaluated over South America by *Chou et al.* [2002] remains in use at CPTEC with the initial soil moisture states in weather and climate simulations interpolated, for a given day, from monthly values in a yearly climatology [*Willmott et al.*, 1985; *Mintz and Serafini*, 1981, 1989, 1992; *Mintz and Walker*, 1993]. This climatology is based on a bucket model [*Manabe*, 1969] with a *Thorntwaite* [1948] estimate of evaporation and prescribed precipitation. However, *Robock et al.* [1998] showed that this climatological data set is substantially different to observations and, more recently, *Goncalves et al.* [2006] compared two SSiB offline runs, one initialized by Mintz and Serafini soil moisture climatology and other by SSiB spin up fields, and found there were significant differences in the calculated latent and sensible heat fluxes, particularly in the semiarid regions of South America.

5. Methods and Analysis

[11] The soil moisture initiations used in the CTR runs were those described in the previous section. Since the bucket model provides only a single soil layer, the total column moisture is interpolated to each of the SSiB three layers in proportion to their depth. The alternative soil moisture initiation (in the SALDAS runs) were calculated using a SSiB-based LDAS system set up over South America (SALDAS) starting from soil moisture states taken from a spin up experiment for the calendar year 2001 [*Goncalves et al.*, 2006], with the SALDAS then continuously forced by the NCEP/GDAS atmospheric forcing through to June 2004. Two 7 day experiments were then conducted using Eta/SSiB in July 2003 and January 2004, i.e., in the Southern Hemisphere summer and winter, respectively. For each month (January and July), the Eta model was run over a period of seven days with a new run initiated each day to give seven independent runs per month. Each run used the soil moisture fields calculated offline (either climatological or derived from SALDAS) as initial conditions and the model provided 72h forecasts with

an output every 24h. Figure 1 is a schematic diagram illustrating the experiment design.

[12] For each 7 day experiment, the 24 hour, 48 hour, and 72 hour forecasts for the CTR and SALDAS runs were compared with daily precipitation and temperature from surface stations and the modeled geopotential height at 500 hPa and the mean sea level pressure with NCEP/GCM analysis fields. Because direct comparison with the limited upper air soundings available and scarce topography-dependent surface observations is problematic, comparison with analyzed NCEP/GCM fields derived from these and other (e.g., remotely sensed) observations is considered preferable. These analyzed fields at least provide a broad measure of the overall behavior of the atmosphere over large areas, such as South America. For the purpose of making comparison, the South American continent was divided into three regions selected on the basis of prevailing weather systems [*Chou et al.*, 2002] and vegetation cover characteristics: the three areas, north (N), northeast (NE), and south (S) as shown in Figure 2.

6. Results

6.1. Initial Soil Moisture States

[13] In general, the differences between the SALDAS and CTR (climatological) soil moisture fields (i.e., volumetric soil moisture in %) in the three soil layers are greater in January 2004, in the wet season, than in July 2003, in the dry season (Figure 3). In January 2004 (Figure 3a), the fractional wetness of the surface layer in the SALDAS initiation field is drier than climatology by up to 0.6 over all of southeastern Brazil, and areas east and west of Amazonia, north of Bolivia, and west of Peru. In the root and deep soil layers, the SALDAS field is drier than climatology in similar areas, although there are significant differences including areas along latitude 10°S in northern Brazil. The SALDAS fields are higher than climatology in all soil layers in the northern portion of the continent, in northeast Brazil and regions east of the Andes in Chile and coastal Peru, and in southern and western Argentina. The differences in the soil wetness in these areas are greatest in the deep soil layer and reach 0.8 in south central Argentina.

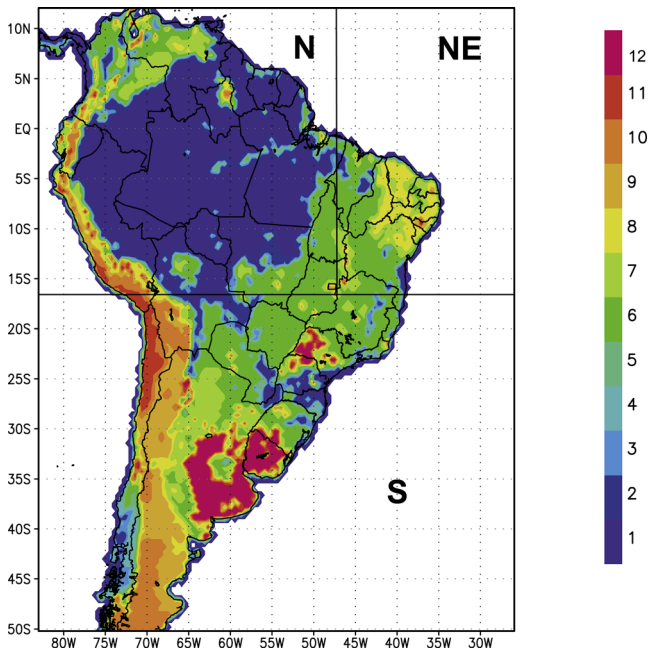


Figure 2. Vegetation cover classification for South America. Type 1 is tropical rain forest; type 2 is broadleaf deciduous trees; type 3 is broadleaf and needleleaf trees; type 4 is needleleaf evergreen trees; type 5 is needleleaf deciduous trees; type 6 is broadleaf trees with ground cover; type 7 is grassland; type 8 is broadleaf shrubs with ground cover; type 9 is broadleaf shrubs with bare soil; type 10 is dwarf trees with ground cover; type 11 is desert; type 12 is crops. The regions where area average analyses were made are N, NE, and S.

[14] In July 2003, the surface layer shows most difference in those areas where the SALDAS field is drier than climatology in all three soils layers. For the surface layer, drier areas include southeast Brazil, northern Amazonia, and the eastern side of the Andes in Bolivia and Peru, with differences ranging from less than 0.2 (in Amazonia and the eastern Andes) to 0.6 (in southeast Brazil). In the root layer, there are differences greater than 0.2 only in small areas of southeastern Brazil while, in the deep soil layer, there are no areas where the SALDAS field is drier than climatology by 0.2. Areas in central Amazonia, north of northeastern Brazil, Argentina, Chile and coastal Peru are where the surface layer in the SALDAS field is wetter than climatology, with differences of up to 0.8. Areas where the SALDAS field is wetter than climatology in the root zone are similar to those for the surface layer, except in central Amazonia (where the differences are small) and in northeastern Brazil where there are more areas with a differences greater than 0.6. The SALDAS field is greater than climatology in the deep soil layer in areas similar to those for the root zone except in central Argentina where difference exceeds 0.8 in some places.

6.2. Gridded Precipitation and Outgoing Long-Wave Radiation

[15] One source of observed precipitation data available for use for comparison with modeled fields in this study is a

$1^\circ \times 1^\circ$ gridded product provided from a collaboration between INMET and CPTEC, which was derived from surface stations distributed over South America interpolated using a modified *Cressman* [1959] scheme [Glahn *et al.*, 1985; Charba *et al.*, 1992]. However, the distribution of surface stations is uneven in South America, and the density of stations is low, especially in the Amazon, the Andes, and central Brazil [Goncalves *et al.*, 2006]. Moreover, the resolution of the interpolated gridded product is coarse compared to the 40 km Eta model resolution. Clearly, this gridded product therefore needs to be used with care.

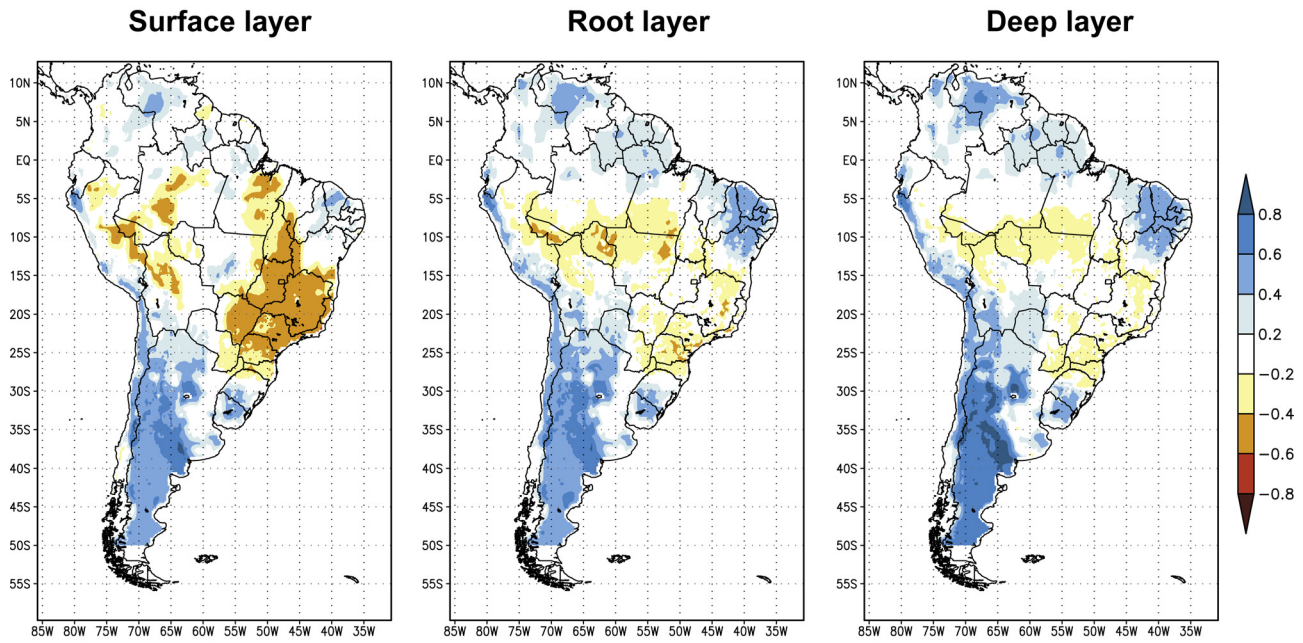
[16] In practice, the main difference in the modeled precipitation in the CTR and LDAS runs is in the amount of precipitation rather than its location. A quantitative comparison between the precipitation fields calculated in the CTR and SALDAS simulations is presented in the next section using in situ (rather than gridded) precipitation observations. In this section, the interpolated precipitation fields described above are used to make a qualitative investigation of the Eta model's ability to simulate the location of the primary precipitation systems. This investigation is aided by use of the observed daily outgoing long-wave radiation (OLR) fields provided by NOAA-CIRES that can be used to identify the approximate location of cloud and, by inference, precipitation.

[17] The observed surface precipitation and daily outgoing long-wave radiation (OLR) fields shown in Figures 4 (left) and 4 (right) for the period 5–12 January 2004 suggest precipitation was associated with two main production mechanisms, namely, (1) precipitation associated with the South Atlantic Convergence Zone (SACZ) [Kodama, 1992; Carvalho *et al.*, 2002] which is here subjectively defined as the zone of enhanced precipitation that extends from the Amazon basin to the South Atlantic Ocean passing above southeastern Brazil [Satyamurty *et al.*, 1998; Liebmann *et al.*, 1998] and (2) convection around 5°N due to the Intertropical Convergence Zone (ITCZ) visible in the outgoing long-wave radiation (OLR) field shown in Figure 4 (right) and observed by surface stations over the northern coast of the continent (Figure 4, left).

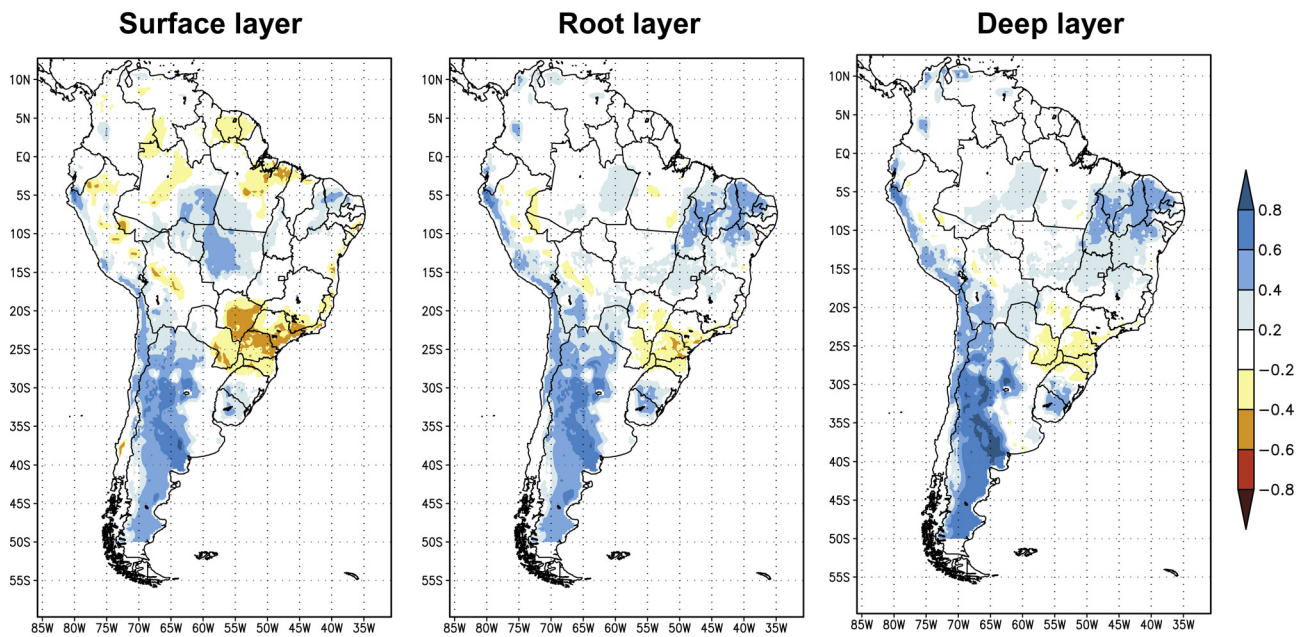
[18] Figure 4 (middle) shows the average Eta 72 hour precipitation forecast during January for the CTR run. The position of the SACZ over the continent was predicted correctly by the CTR run although the LDAS run provided a slightly better prediction of the location of the system. In the next section it is shown that the LDAS run also compares better with surface observations of precipitation.

[19] Figure 5a shows the difference in precipitation between the SALDAS and CTR runs for the 72 hour forecasts in January 2004. The alternating pattern of differences over southeastern Brazil, which are oriented along the SACZ axis indicate that the fields are out of phase (shifted) rather than having different magnitude. In fact, the forecasts initialized by the SALDAS soil moisture fields positioned the SACZ slightly south of CTR forecasts for the reasons described below.

[20] Studies [e.g., Ferreira *et al.*, 2004] have shown that the mechanisms that regulate precipitation over South America during the wet season can be better understood if upper and lower troposphere dynamics are considered separately. Many mechanisms influence large-scale circulation over South America, including tropical heating [Silva



(a) January (SALDAS – CPTEC)



(b) July (SALDAS – CPTEC)

Figure 3. Difference (a) in January 2004 and (b) in July 2003 between the SALDAS and CTR initial soil moisture fraction (in the range 0 to 1), for the (left) surface layer, (middle) root zone, and (right) deep soil layer.

Dias et al., 1983; Gandu and Geisler, 1991], extratropical convection [Bellassiano, 2000], and convection over remote areas such as the western and central Pacific and Africa [Gandu and Silva Dias, 1998]. For the period studied here, the main regional features of upper tropospheric circulation are the Bolivian High (BH), that can be defined as a middle/upper level warm core anticyclone due to radiational heating and latent heat release during intense convection [Virji,

1981], the cyclonic vortex in the vicinity of northeast Brazil (CVNE) [Kousky and Gan, 1981; Mishra et al., 2001], and the climatological midlatitude trough (CT) located over southeastern Brazil. The CT occurs from November to March and splits the Subtropical Ridge into two parts, one over South America, the other over Africa. Flow between the CT and BH contributes to precipitation in the region by bringing surface and upper level disturbances into the area.

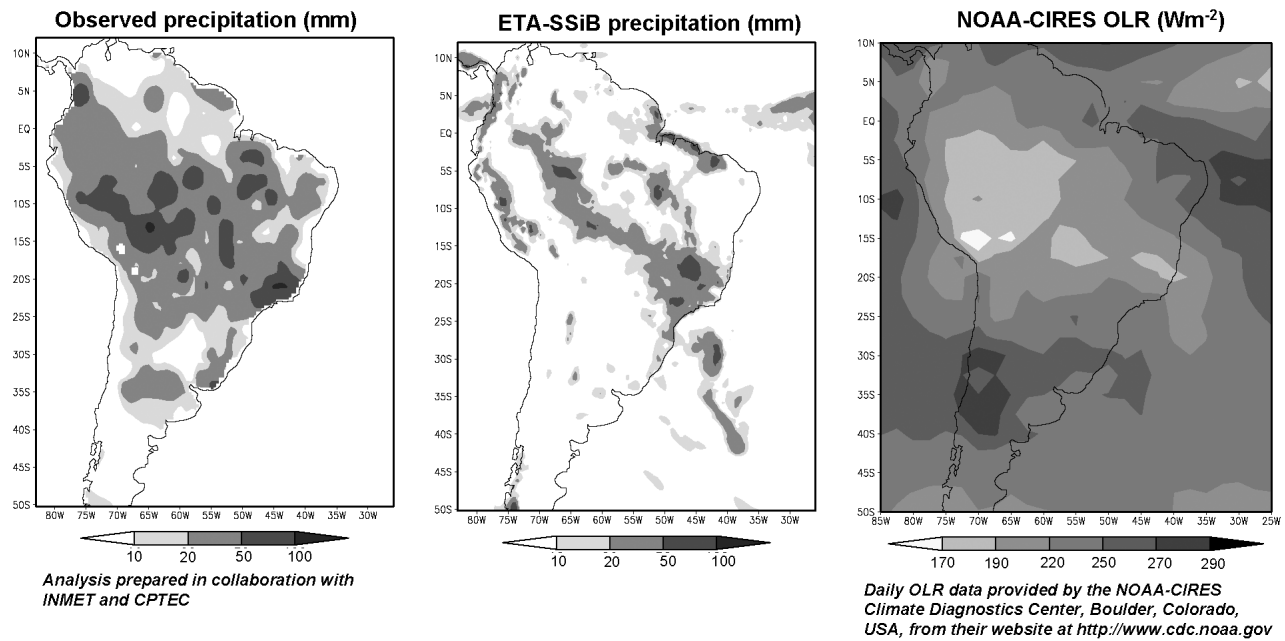


Figure 4. For January 2004, (left) interpolated surface observations of precipitation, (middle) 72 hour Eta-SSiB precipitation forecast, and (right) outgoing long-wave radiation (OLR).

Thus the position of the BH plays an important role in determining the location and intensity of precipitation over most of the continent, including the SACZ.

[21] The authors suggest that an increase in the latent heat flux in the northern Argentina and Paraguay and southern Bolivia, where SALDAS initial soil conditions are moister than the CTR initiation may cause a southward shift in the predicted SACZ through a dynamical connection with the BH in the upper troposphere. Figure 5b shows the difference in the latent heat flux between the SALDAS and CTR runs in January, clearly showing the regions with higher

differences are in the semi arid northeast of Brazil (where there were no significant changes in the atmospheric circulation and precipitation) and northern Argentina and Paraguay and southern Bolivia. Increased latent heat in the region with the SALDAS moister conditions cause a net increase in the atmospheric temperature between 1000 hPa and 500 hPa, causing the Eta model to predict the warm core of the BH to be shifted further west in comparison with the CTR run. Consequently, the CT trough in the SALDAS run (and the associated divergence in the upper levels) is predicted to be further to the southwest of the CT than in the

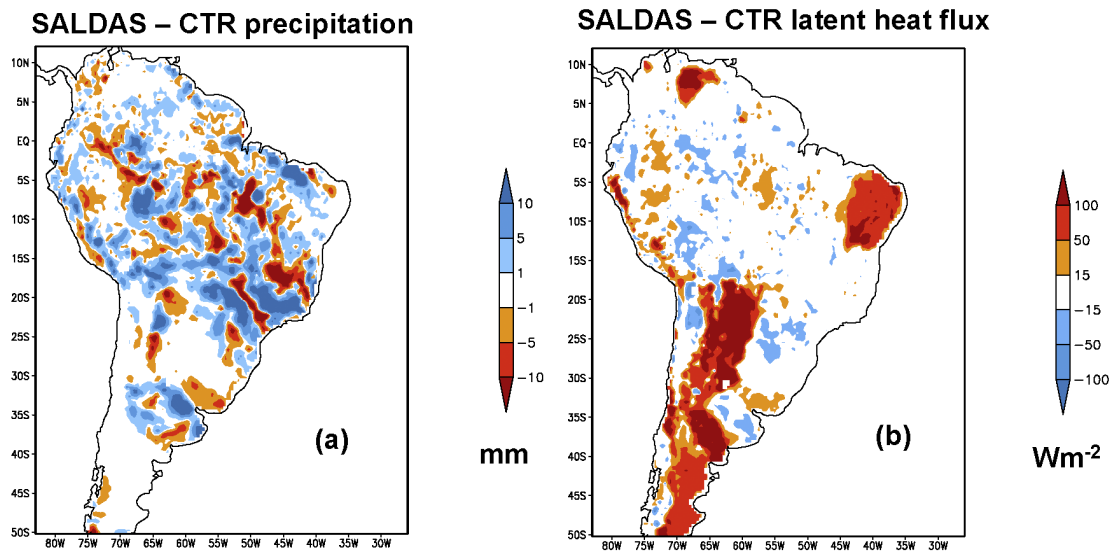


Figure 5. Difference between 72 hour Eta model forecasts in January 2004 when using the SALDAS initiation relative to when using the CTR initiation for (a) time-averaged precipitation in mm and (b) time-averaged latent heat in Wm^{-2} .

January 2004 250 hPa streamlines

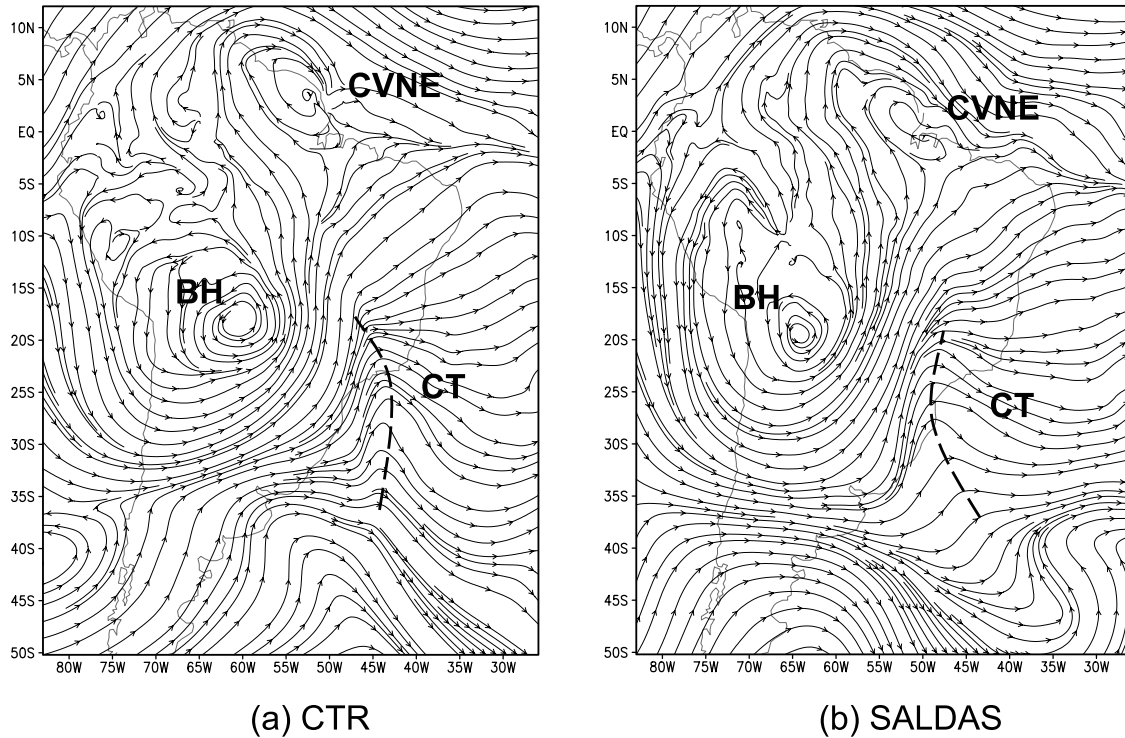


Figure 6. Time-averaged streamlines at 250 hPa in 72 hour Eta model Eta forecasts for January 2004 (a) for the CTR initiation and (b) for the SALDAS initiations, illustrating the location of the main upper troposphere circulation patterns, namely, the Bolivia High (BH), the cyclonic vortex over Brazil northeast (CVNE), and the Atlantic Trough (CT). Note that CT is indicated as a dashed line.

CTR run, displacing the low-level convergence (SACZ) southward. Figure 6 shows the 250 hPa streamlines for the CTR run (Figure 6a) and for the SALDAS run (Figure 6b) along with the main circulation patterns (BH, CT and CVNE).

[22] The BH configuration in the Eta forecasts initialized by the SALDAS fields also causes a change in the upper troposphere circulation over southern South America, with a second trough (associated with a new frontal system) predicted to southwest of its position in CTR run, and therefore modifying the precipitation pattern between 30S and 40S. There is also the local influence of the convective activity of the region due to the higher latent heat flux between 35S and 40S (Figure 5b) in the SALDAS initialization.

[23] Over the Amazon region, the change in the upper troposphere circulation also resulted in a net increase in the convergence at 250 hPa (not shown) in the SALDAS run in comparison with the CTR run, suggesting a decrease in the precipitation generated by deep convection.

[24] Figure 7 shows similar results for the drier period of 3–10 July 2003. The observed average precipitation mainly occurs in three regions: southern Brazil, south of Chile, and in the northernmost region of the continent associated with convection in the ITCZ, which is located further north than it is in January. In the southern region, precipitation is produced, mainly, by frontal systems and topographic effect, and the Eta-SSib model was able to simulate the

position of this precipitation correctly. The model does seem to predict the position of maximum intensity in the ITCZ a few degrees south of observations, although model results in this area may be influenced by the boundary conditions of the domain which are updated every 6 hours. In the South Atlantic, minimum values of OLR agree with the position of frontal precipitation predicted by the Eta-SSiB model over southeast Brazil and near ocean. However, the model was not able to capture the (albeit limited) precipitation near the coast of northeast Brazil that may be caused by easterly waves, which common in this area June, July, and August. The precipitation in the SALDAS and CTR runs show small differences, and these are mostly in the amount rather than the position of the systems during this period. An analysis of the quantitative differences between the two runs is given in the next section.

6.3. Equitable Threat Score and Bias

[25] The equitable threat score (ETS) measures the ability of the model to predict the area with precipitation above a given threshold [Anthes *et al.*, 1989; Mesinger, 1996]. It is defined as:

$$ETS = \frac{H - CH}{F + O - H - CH} \quad (1)$$

where F is the number of points the model predicts above a specified threshold, O is the number of observations above

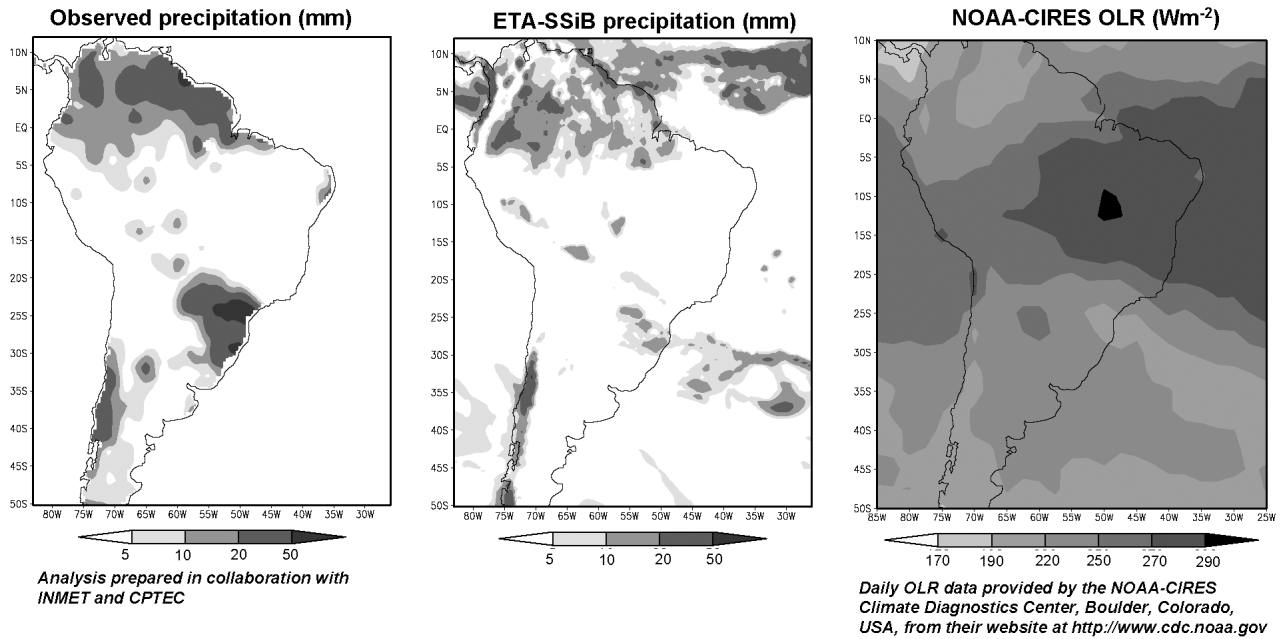


Figure 7. For July 2003, (left) interpolated surface observations of precipitation, (middle) 72 hour Eta-SSiB precipitation forecast, and (right) outgoing long-wave radiation (OLR).

the same threshold, H is the number of model “hits”, CH is the number of points corresponding to random “hits”, calculated from

$$CH = \frac{F \times O}{N} \quad (2)$$

where N is the number of points in the verification domain. In this study, the ETS was calculated for the following precipitation thresholds: $P = 0$ mm, $P > 0$ mm, $P > 5$ mm, $P > 10$ mm, $P > 15$ mm, $P > 20$ mm, $P > 30$ mm, and $P > 50$ mm.

[26] The bias score is defined as

$$BIAS = \frac{F}{O} \quad (3)$$

[27] ETS varies from 0 to 1, with higher values indicating better simulations and ETS and BIAS are used in combination and a perfect simulation would be equivalent to $ETS = 1$ and $BIAS = 1$.

[28] The main interest of this study was to investigate relatively changes in model performance. Consequently, percentage change in the ETS and BIAS are calculated for the N, NE and S regions shown in Figure 2 when using the SALDAS initiation relative to when using the CTR initiation. Recognizing that performance is better when ETS and BIAS approaches unity, the percentage change in ETS, is give by

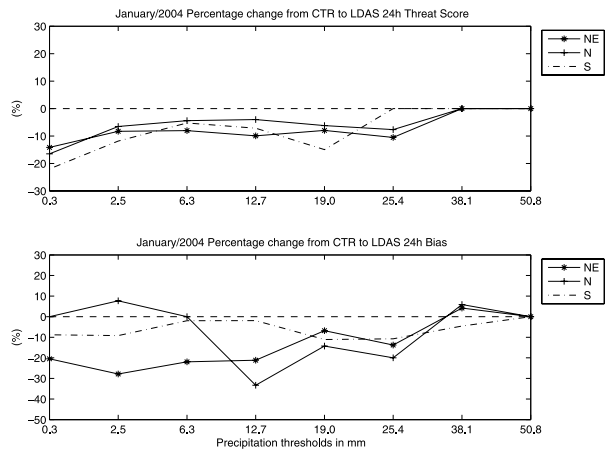
$$PC_{ETS} = 100 \times \frac{|ETS_{SALDAS} - 1| - |ETS_{CTR} - 1|}{|ETS_{SALDAS} - 1|} \quad (4)$$

while the percentage change in the BIAS score is calculated from:

$$PC_{BIAS} = 100 \times \frac{|BIAS_{SALDAS} - 1| - |BIAS_{CTR} - 1|}{|BIAS_{SALDAS} - 1|} \quad (5)$$

Note the sign of the BIAS is not being considered, rather how close its value is to unity.

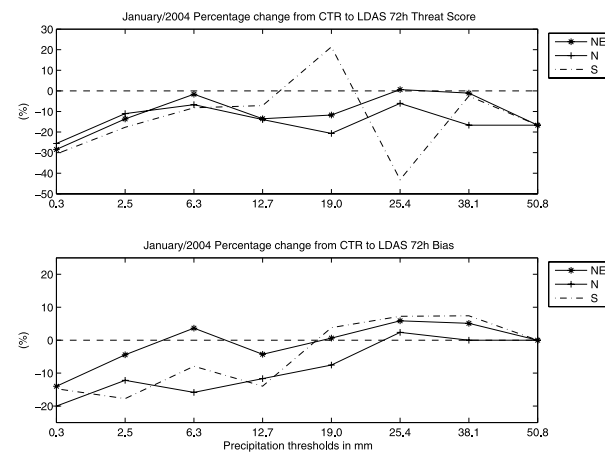
[29] Figure 8a shows the percentage change in the 24h ETS (Figure 8a, top) and BIAS (Figure 8a, bottom) in January 2004 in the NE (line with stars), N (line with crosses), and S (dashed line) areas for the different precipitation thresholds shown on the x axis (in mm). Note that negative values of ETS imply an increase in the model performance when using the SALDAS initialization rather than the climatological initiation. In the 24 hour forecast, the SALDAS initialization results show a better ETS than does CTR initiation for all regions, with up to 23% improvement for light precipitation, and up to 10% for all the others thresholds. In the case of the BIAS (Figure 8a, bottom), for precipitation values up to 6.3 mm there is a degradation in the forecast for the N region, but in the NE there is a 25% increase in the performance and in the S the performance increases by up to 8%. For the thresholds above 6.3 mm, there is an improvement in all regions up to a threshold on 38 mm when there is a degradation of 5% in the N and NE areas. In Figure 3a, the most significant differences in the soil moisture in the N region are found in the surface layer (the SALDAS is dryer than CTR) suggesting that in the first hours of simulation evapotranspiration may be partially inhibited, therefore reducing precipitation (i.e., increasing the occurrence of light precipitation) which would degrade the BIAS at low thresholds. However, the moisture in the shallow surface layer will rapidly adjust so the effect is mainly in the first 24h precipitation forecasts.



NE	958	605	383	183	115	075	031	015
N	585	415	241	118	075	057	024	010
S	1330	841	518	285	159	090	033	007

Number of observations

(a)



NE	1179	835	547	303	189	107	040	019
N	520	346	190	097	083	042	019	009
S	1295	871	542	288	165	099	030	011

Number of observations

(b)

Figure 8. (a) Percentage change in the 24 hour forecast (top) ETS and (bottom) BIAS in January 2004, in NE (line with stars), N (line with crosses), and S (dashed line) for the different precipitation thresholds shown on the x axis (mm). (b) Percentage change in the 72 hour forecast (top) ETS and (bottom) BIAS in January 2004 in NE (line with stars), N (line with crosses), and S (dashed line) for the different precipitation thresholds shown on the x axis (mm).

[30] Figure 8b is similar to Figure 8a but shows the results for the 72 hour forecast in the same month (January). In general, the percentage change in ETS shows increased performance (Figure 8b, top) although the picture is less consistent for the increased forecast lead time. There is an increase performance in the range 0–25% in the N and NE regions. In the S region, there is a maximum decrease in performance of 20% for the

19 mm threshold and a maximum increase in performance of 45% for the 25.4 mm threshold. In the case of the BIAS, there is a 5% decrease in performance for the NE region for thresholds of 6.3 mm, 25.4 mm and 38.1 mm, but an 12% increase in performance for the 0.3 mm threshold. In the N and S areas, the behavior is broadly similar, with increased performance of 15% and 20%, respectively, for the 0.3 mm threshold, but then progressively less improvement at higher thresholds, and degraded performance for thresholds above 19 mm.

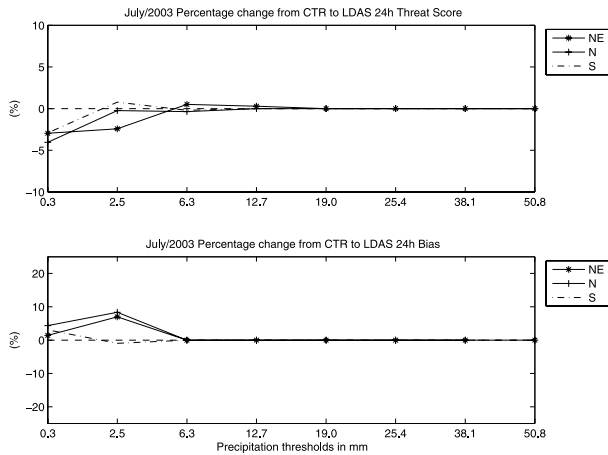
[31] The ETS and BIAS performance analysis for the Eta-SSiB model for the drier month of July 2003 is shown in Figure 9a for the 24 hour forecast and in Figure 9b for the 72 hour forecast. Because precipitation is generally low across the whole continent in this month, only precipitation thresholds less 19 mm threshold are significant. For thresholds lower than 2.5 mm, the 24 hour forecasts show an improvement of up to 5%. For thresholds up to 6.3 mm (light rain) there is a 5% improvement in the NE area, and 3% in the other areas. In the case of the ETS, in all regions there was less than 1% degradation in performance for thresholds of 6.3 and 12.7 mm. In the case of the BIAS, the 24 hour forecast showed degradation of up to 10% in all regions for thresholds up to 6.3 mm. For the 72 hour forecast (Figure 9b), in the NE area there is a performance increase in the ETS performance of 18% and 30% for the 0.3 mm and 2.5 mm thresholds, but a degradation of 20% for a 25.4 mm threshold. The BIAS was improved for thresholds lower than 6.3 mm for in 72 hour forecast for July 2003, but degradation for higher thresholds.

6.4. Surface Temperature

[32] Temperature comparisons are made using the 2 m modeled temperature from Eta-SSiB, this being the height closest to that at which temperature observations are usually made at climate stations. The modeled temperatures were interpolated to locations where observations were available, the difference taken, and contours drawn (Figure 10). Figure 10a shows that the average temperature in January 2004 exhibits little variation for latitudes north of 15°S, the value is close to 28°C except over the Andes where the values drop rapidly with altitude. As might be expected, the temperature also falls further south near the coast in southeastern Brazil (24°C) and in Argentina where the values fall off with latitude.

[33] In general, the CTR runs calculate a temperature that is 2°C colder than the observations across the continent, except for a small area in northeast Brazil, where it is 2°C warmer, and along the east coast south of 25°S, where it is up to 6°C colder than observations. The SALDAS run calculates temperatures that show a larger area with 6°C difference near the coast of southeastern Brazil, and 4°C colder than observed areas in the northeast and north of the continent.

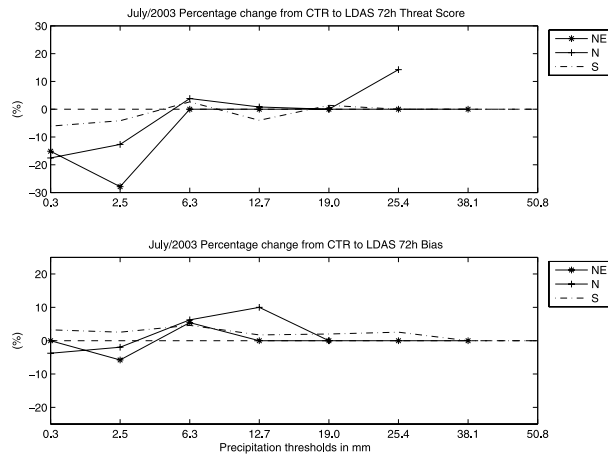
[34] For July 2003, Figure 11b shows that both the CTR and SALDAS runs are (on average) 4°C colder than observations for latitudes lower than 25°S. For some areas in northeast Brazil and in the northern part of the continent, the differences in both simulations are of up to 6°C colder. The low temperatures over the semiarid northeast Brazil can be explained by the nighttime radiative cooling



NE	172	097	047	025	017	012	005	003
N	238	144	070	015	007	005	002	0
S	425	208	097	053	030	015	010	005

Number of observations

(a)



NE	192	092	041	011	006	003	001	0
N	282	174	092	017	005	001	0	0
S	505	250	145	092	057	040	021	0

Number of observations

(b)

Figure 9. (a) Percentage change in the 24 hour forecast (top) ETS and (bottom) BIAS in July 2003 in NE (line with stars), N (line with crosses), and S (dashed line) for the different precipitation thresholds shown on the x axis (mm). (b) Percentage change in the 72 hour forecast (top) ETS and (bottom) BIAS in July 2003 in NE (line with stars), N (line with crosses), and S (dashed line) for the different precipitation thresholds shown on the x axis (mm).

due to the low cloud cover (shown by the high values of OLR) and the presence of broadleaf shrub as ground cover (Figure 2).

[35] Figure 12 shows the difference in the surface temperature between runs with SALDAS and CTR initializations for 72 hour forecasts in January 2004 (Figure 12a) and in July 2003 (Figure 12b). As expected,

in the regions where SALDAS initiation is moister than CTR, the temperatures are cooler, i.e., in northeast Brazil, central and southern regions of the continent in January, and northeast Brazil, the central continent and along the east coast from northern Chile to Peru in July. The cooler temperatures result from the partitioning between sensible and latent heat in the areas where the SALDAS is moister: there is an increase in the latent heat flux and a equivalent decrease in the sensible heat, thus cooling the near surface atmosphere. The CTR is significantly moister than SALDAS only in southeast Brazil in January (Figure 2a) and southern Brazil in July (Figure 2b). However, these differences occur in the thin surface layer which adjusts in the first hours of the run, with little influencing in longer forecasts (e.g., 72h predictions).

6.5. Geopotential Height and Mean Sea Level Pressure

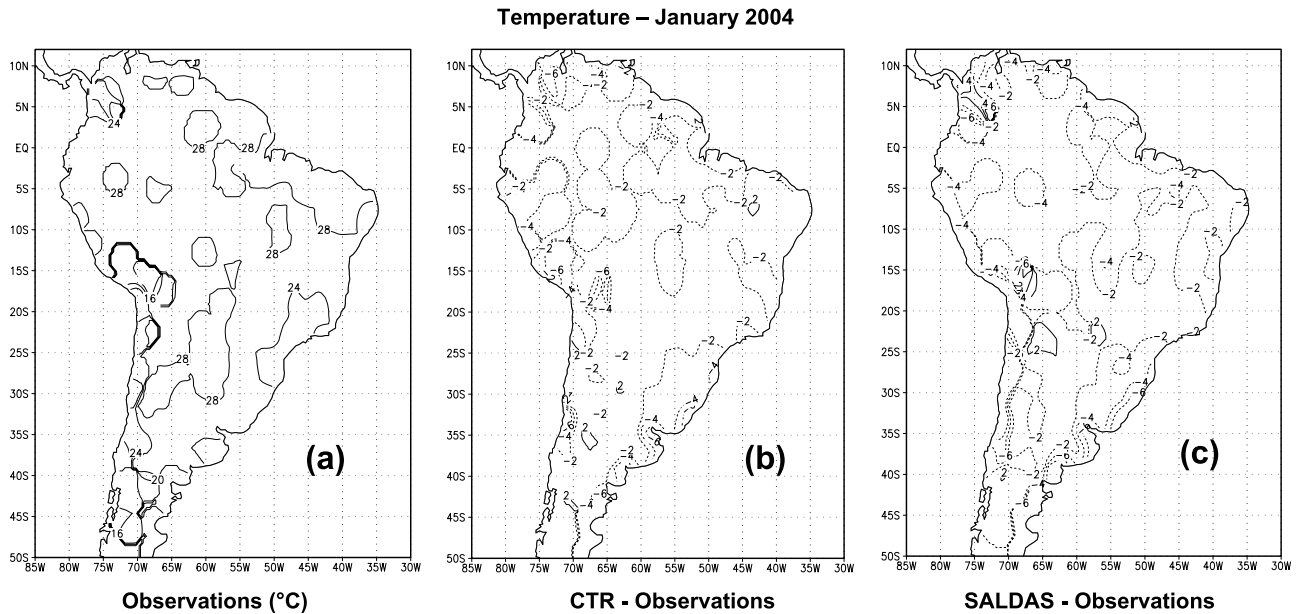
[36] Over each area (N, NE, and S), the area-averaged RMSE for the geopotential height at 500 hPa and mean sea level pressure were calculated between the CTR and SALDAS simulations and the NCEP analysis. The results were then compared as the percentage change in order to diagnose the improvement or degradation in the RSME for the SALDAS runs relative to the CTR runs. The percentage change (PC; %) in each case was calculated from

$$PC = \frac{RMSE_{SALDAS} - RMSE_{CTR}}{RMSE_{SALDAS}} \times 100 \quad (6)$$

[37] Table 1 shows the percentage change in RMSE for geopotential height at 500 hPa and the mean sea level pressure in January 2004 and July 2003 for the 24 hour, 48 hour, and 72 hour forecasts. Negative values mean the errors in the SALDAS run are lower than the errors in the CTR run.

[38] In January 2004, the percentage change in geopotential height is negative for all forecast periods in the N and S regions. In NE region, there are small percentage changes (less than unity) in the 24 hour forecast but the RMSE for the SALDAS 48 hour run is approximately 7% higher than for the CTR run. The maximum percentage change occurs for the 72 hour run in the N region where RMSE for the CTR run is 53% higher than for SALDAS run. The RMSE for the mean sea level pressure for the CTR run is higher than for the SALDAS run for all regions and forecast periods in January 2004, and the differences increase as the forecast hours increase, with a maximum percentage change of 32% for the 72 hour run in the S region.

[39] In July 2003, the percentage change in the RMSE of geopotential height is small and positive in all areas for the 24 hour forecast period. In the NE and S the maximum percentage change (-9% and -2.6%, respectively) occurs for the 48 hour forecast period while, in the N region, the maximum percentage change (2.8%) is for the 24 hour forecast period. For the mean sea level pressure, the percentage change in RMSE values decreases as the forecast period increases for all regions. For the mean sea level pressure, there is just one occurrence of a positive percentage change (~1%) for the 24 hour forecast in the N region, while the maximum improvement resulting from use of the



Analysis prepared in collaboration with INMET and CPTEC

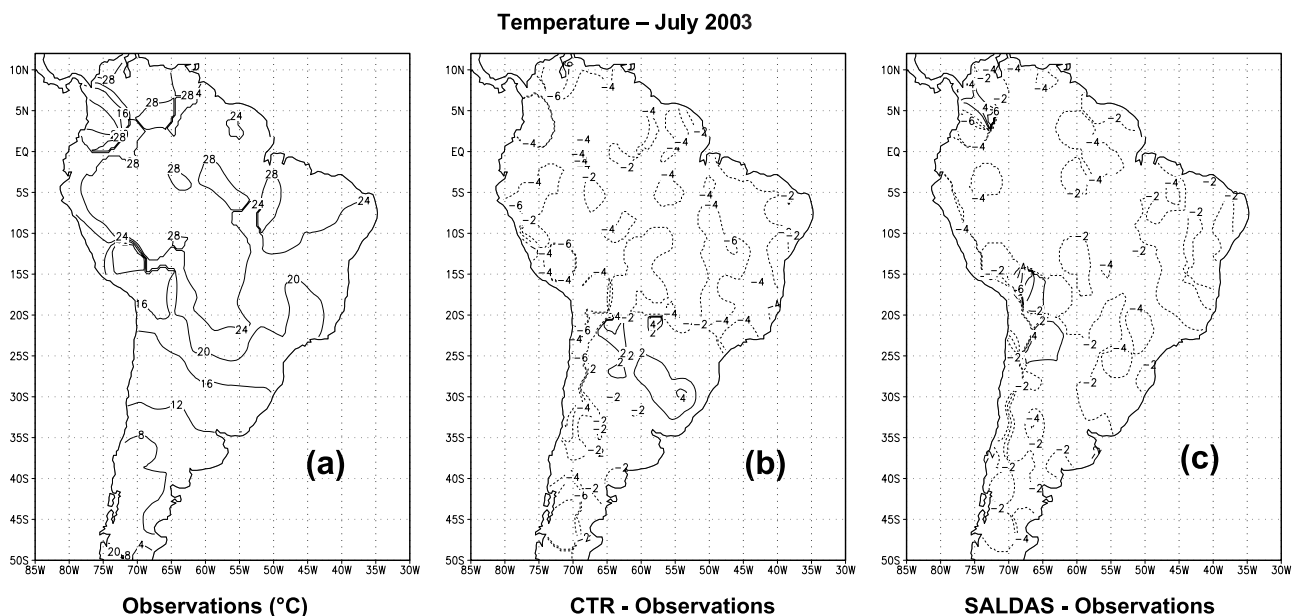
Figure 10. (a) Observed surface temperature and differences (b) between the temperature calculated in the CTR run and observations and (c) between the temperature calculated in the SALDAS run and observations for the 72 hour forecasts in January 2004.

SALDAS fields is a percentage change of 18.6% in the NE region for the 72 hour forecast.

7. Summary and Conclusions

[40] In this study, the Eta model coupled to SSiB was run over South America with a grid resolution of 40 km and

with boundary and initial conditions taken from NCEP analysis. The model was initialized using two different soil conditions; one, the soil moisture climatology used operationally at CPTEC; the other, the product of a 3 year LDAS run using SSiB forced by the GLDAS atmospheric fields. Two 7 day runs were performed during the austral winter



Analysis prepared in collaboration with INMET and CPTEC

Figure 11. (a) Observed surface temperature and differences (b) between the temperature calculated in the CTR run and observations and (c) between the temperature calculated in the SALDAS run and observations for the 72 hour forecasts in July 2003.

SALDAS-CTR Time-averaged surface temperature differences

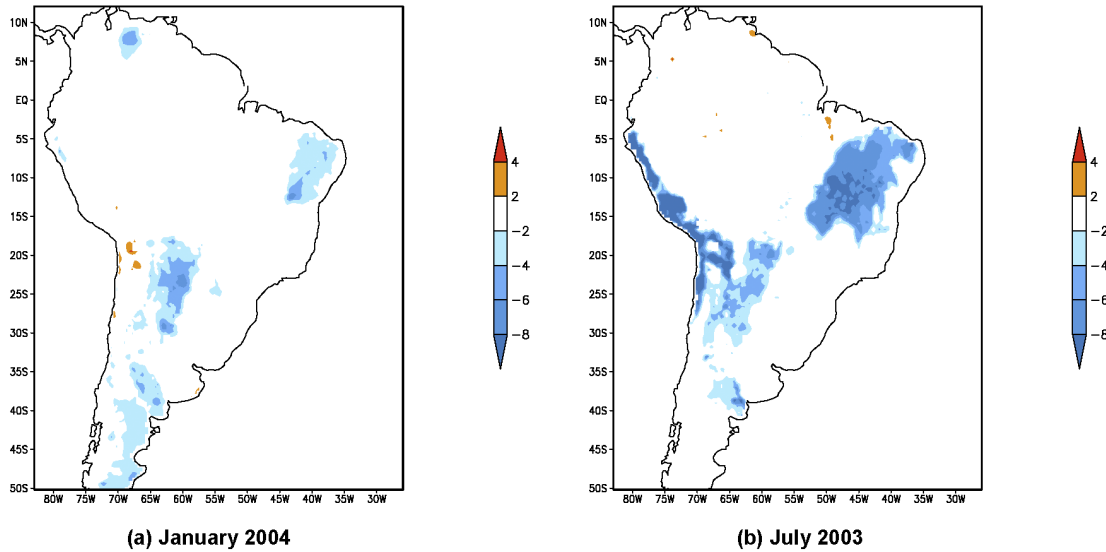


Figure 12. SALDAS-CTR difference in the time-averaged 72 hour surface temperature forecasts in °C for the SALDAS initiation relative to the CTR initiation for (a) January 2004 and (b) July 2003.

(the dry season, in July 2003) and summer (the wet season, in January 2004) with these alternative initial soil moisture conditions. The resulting forecasts of up to 72 hours were compared against each other and against observations.

[41] The CTR soil moisture fields were, on average, drier than the SALDAS soil moisture fields in both January and July in northeastern Brazil, the inner continent, southern portions of Amazonia, and in a region that extends from southern Argentina to northern of Peru, with increasingly greater differences at greater depth. In January, the SALDAS soil moisture fields are drier than the CTR fields in the inner continent and southeastern Brazil, especially in the surface layer. Regardless of which initial soil moisture fields were used, the Eta model was able to predict the general location of precipitation in both seasons reasonably well. In particular, the model correctly predicted the convective band from Peru to southeast Brazil and correctly located the ITCZ in January. In July, the Eta-SSiB misplaced the precipitation associated with the ITCZ to some extent compared to OLR fields, but this may be due to the influence of the model’s lateral boundary conditions. The

increase in the latent heat flux over north of Argentina, Paraguay and Bolivia in the SALDAS initialization caused an increase in the lower troposphere temperature and as consequence the Eta-SSiB model predicted the BH (a warm core upper tropospheric cyclonic vortex) west of the CTR predictions, shifting the SACZ southward. Nonetheless, the Eta-SSiB model generally did predict the position of the precipitation correctly over the continent quite well in July although, when compared to the measured OLR, it appeared to displace the convection associated with the frontal systems southward.

[42] In January 2004, a quantitative analysis of model precipitation against station observations shows that the SALDAS initialization yields a better ETS than the CTR initiation for the 24 hour forecast for all regions, with up to 23% improvement for light precipitation and up to 10% improvement for all others thresholds. There is degradation of the BIAS for light precipitation in the N region, but improvement in all other regions. With the SALDAS initialization, the 72 hour forecasts also show an overall increase in ETS performance of 20% in all regions and for

Table 1. Percentage Change in the RMSE for Geopotential Height at 500 hPa and Mean Sea Level Pressure Between the SALDAS and the CTR Computed for Each Region (N, NE and S) for the 24, 48, and 72 hour Forecast Periods^a

	Geopotential Height at 500 hPa			Mean Sea Level Pressure		
	NE	N	S	NE	N	S
January						
24h	0.911	-0.74	-0.03	-7.95	-0.04	-2.18
48h	7.08	-2.11	-15.22	-0.31	-6.34	-11.66
72h	-10.26	-53.45	-10.94	-19.24	-22.89	-31.24
July						
24h	0.41	2.81	0.43	-0.26	1.01	-0.58
48h	-9.51	-2.59	-2.63	-8.28	-11.69	-7.29
72h	-8.98	-1.7	0.18	-18.66	-15.97	-14.64

^aThe percentage change is calculated for January 2004 and July 2003. Negative values imply RMSE for the CTR run is higher than for the SALDAS run.

all thresholds. For the same forecast period, there is an average increase in performance for BIAS of 10% for thresholds lower than 19 mm but degradation in performance above this threshold. Because precipitation is low in July, only the precipitation events below the 19 mm threshold are significant. For the 24 hour forecasts, there was an improvement of 3% in the ETS and a degradation of around 5% in BIAS for all regions when the SALDAS initiation fields were used. For the 72 hours forecasts, there was an improvement of up to 30% in the ETS in the N region, but a degradation of around 5% in the BIAS.

[43] The differences between modeled surface temperatures and observations are similar for both initiation fields and, on average, about 2°C colder in January and 4°C colder in July. The SALDAS runs have larger areas with temperatures colder than the CTR runs in January, particularly near the east coast in southern Brazil and Argentina. In July, the CTR run is colder than the SALDAS run in semiarid and desert areas where the initial soil moisture is drier and there is greater nighttime radiative cooling. When comparing the surface temperature predictions between the two runs, the areas where SALDAS initial soil moisture fields are moister than CTR show lower temperatures due to an increase in the latent heat flux in the energy partitioning.

[44] The 500 hPa geopotential height and mean sea level pressure analysis show a general improvement in the performance of the model of up to 53% (in the N area) when initialized by SALDAS soil moisture fields. Whenever there is degradation of performance in predicting the geopotential height or mean sea level pressure, the percentage change is less than 10%.

[45] In conclusion, the Eta-SSiB showed a general overall improvement in performance for all the variables analyzed in this study (precipitation, surface temperature, geopotential height, and mean sea level pressure) when initialized by the SALDAS rather than the CTR soil moisture fields. However, a more detailed small-scale analysis is justified for the limited regions where using SALDAS fields degrades the model simulation in the present study, including areas in northeastern Brazil and some southern areas where the SALDAS fields are wetter than the CTR fields. Further investigation of whether there are more significant differences in the mesoscale atmospheric circulations modeled by the Eta model operating at 40 km resolution is also justified.

[46] **Acknowledgments.** Primary support for this research came from NASA project NAG5-9796. Additional support for W. James Shuttleworth came from the NASA-LBA Ecology Program (Group CD18) under grant NCC5-709 and from SAHRA (the NSF Center for Sustainability of semi-Arid Hydrology and Riparian Areas) under grant EAR9876800. The authors wish to acknowledge the help of the staff at CPTEC for promptly providing the data used in this research. Thanks also go to the GLDAS team at the NASA GSFC (Hydrology Sciences Branch, code 614.3) for the support on setting up LDAS over South America and to the NASA Postdoctoral Program.

References

- Anthes, R. A., Y.-H. Kuo, E.-Y. Hsie, S. Low-Nam, and T. W. Bettge (1989), Estimation of skill and uncertainty in regional numerical models, *Q. J. R. Meteorol. Soc.*, *115*, 763–806.
- Arakawa, A., and V. R. Lamb (1977), Computational design of the basic dynamical process of the UCLA general circulation model, *Methods Comput. Phys.*, *17*, 173–265.
- Bellassiano, M. (2000), Study of tropical heat sources impact (in Portuguese), M.S. dissertation, 73 pp., Inst. Astron. e Geofisicutes, Univ. de São Paulo, São Paulo, Brazil.
- Betts, A. K. (1986), A new convective adjustment scheme, part I: Observational and theoretical basis, *Q. J. R. Meteorol. Soc.*, *112*, 677–691.
- Betts, A. K., and M. J. Miller (1986), A new convective adjustment scheme, part II: Single column model tests using GATE wave, BOMEX, and Arctic air-mass data sets, *Q. J. R. Meteorol. Soc.*, *112*, 693–709.
- Bonatti, J. P. (1996), Modelo de circulação geral atmosférico do CPTEC, in *Climanálise Especial (10 anos Edicao Especial)*, 5 pp., Cent. de Previsão de Tempo e Estud. Climáticos, Cachoeira Paulista, Brazil. (Available at <http://tucupi.cptec.inpe.br/products/climanalise/cliesp10a/bonatti.html>)
- Bryan, K. (1969), A numerical method for the study of the circulation of the World Ocean, *J. Comput. Phys.*, *4*, 347–376.
- Carvalho, L., C. Jones, and B. Liebmann (2002), Extreme precipitation events in southeastern South America and large-scale convective patterns in the South Atlantic Convergence Zone, *J. Clim.*, *15*, 2377–2394.
- Charba, J. P., A. W. Harrell III, and A. C. Lackner III (1992), A monthly precipitation amount climatology derived from published atlas maps: Development of a digital database, *TDL Off. Note 92-7*, 20 pp., Natl. Weather Serv., Silver Spring, Md.
- Chou, S. C., A. M. B. Nunes, and I. F. A. Cavalcanti (2000), Extended forecasts over South America using the regional Eta model, *J. Geophys. Res.*, *105*, 10,147–10,160.
- Chou, S. C., C. A. S. Tanajura, Y. Xue, and C. A. Nobre (2002), Simulation of the coupled Eta/SSiB model over South America, *J. Geophys. Res.*, *107*(D20), 8088, doi:10.1029/2000JD000270.
- Cressman, G. F. (1959), An operational objective analysis system, *Mon. Weather Rev.*, *87*, 367–374.
- Crow, W. T., and E. F. Wood (2003), The assimilation of remotely sensed soil brightness temperature imagery into a land-surface model using ensemble Kalman filtering: A case study based on ESTAR measurements during SGP97, *Adv. Water Resour.*, *26*, 137–149.
- de Goncalves, L. G. G., W. J. Shuttleworth, E. J. Burke, M. Rodell, P. R. Houser, D. L. Toll, and K. Arsenault (2006), Toward a South American Land Data Assimilation System (SALDAS): Aspects of land surface model spin-up using the Simplified Simple Biosphere (SSiB), *J. Geophys. Res.*, doi:10.1029/2005JD006297, in press.
- Fennessy, M., and J. Shukla (2000), Seasonal prediction over North America with a regional model nested in a global model, *J. Clim.*, *13*, 2605–2627.
- Ferreira, N. J., A. A. Correia, and M. C. V. Ramirez (2004), Synoptic scale features of the tropospheric circulation over tropical South America during WETAMC TRMM/LBA experiment, *Atmosfera*, *17*, 13–30.
- Findell, K. L., and E. A. B. Eltahir (2003a), Atmospheric controls on soil moisture—Boundary layer interactions. Part I: Framework development, *J. Hydrometeorol.*, *4*, 552–569.
- Findell, K. L., and E. A. B. Eltahir (2003b), Atmospheric controls on soil moisture—boundary layer interactions. Part II: Feedbacks within the continental United States, *J. Hydrometeorol.*, *4*, 570–583.
- Gandu, A. W., and J. E. Geisler (1991), A primitive equations model study of the effects of topography on the summer circulation over tropical South America, *J. Atmos. Sci.*, *48*, 1822–1836.
- Gandu, A. W., and P. L. Silva Dias (1998), Impact of tropical heat sources on the South American tropospheric upper circulation and subsidence, *J. Geophys. Res.*, *103*, 6001–6015.
- Giorgi, F., and L. O. Mearns (1999), Introduction to special section: Regional climate modeling revisited, *J. Geophys. Res.*, *104*, 6335–6352.
- Glahn, H. R., T. L. Chambers, W. S. Richardson, and H. P. Perrotti (1985), Objective MAO analysis for the local AFOS MOS Program, *Tech. Memo. NWS TDL 75*, 34 pp., NOAA, Silver Spring, Md.
- Houser, P. R., W. J. Shuttleworth, H. V. Gupta, J. S. Famiglietti, K. H. Syed, and D. C. Goodrich (1998), Integration of soil moisture remote sensing and hydrologic modeling using data assimilation, *Water Resour. Res.*, *34*(12), 3405–3420.
- Janjic, Z. I. (1990), The step-mountain coordinate: Physical package, *Mon. Weather Rev.*, *118*, 1429–1443.
- Janjic, Z. I. (1994), The step-mountain Eta coordinate model: Further developments of the convection, viscous sublayer and turbulence closure schemes, *Mon. Weather Rev.*, *122*, 927–945.
- Kanamitsu, M., C.-H. Cheng-Hsuan, J. Schemm, and W. Ebisuzaki (2000), The predictability of soil moisture and near-surface temperature in hindcasts of the NCEP seasonal forecast model, *J. Clim.*, *16*, 510–521.
- Kodama, Y.-M. (1992), Large-scale common features of subtropical precipitation zones (the Baiu frontal zone, the SPCZ, and the SACZ), part I: Characteristics of subtropical frontal zones, *J. Meteorol. Soc. Jpn.*, *70*, 813–835.
- Koster, R. D., M. J. Suarez, and M. Heiser (2000), Variance and predictability of precipitation at seasonal-to-interannual timescales, *J. Hydrometeorol.*, *1*, 26–46.
- Kousky, V. E., and M. A. Gan (1981), Upper tropospheric cyclonic vortices on the tropical South Atlantic, *Tellus*, *33*, 538–551.

- Liebmann, B., J. A. Marengo, J. D. Glick, V. E. Kousky, I. C. Wainer, and O. Massambani (1998), A comparison of rainfall, outgoing longwave radiation and divergence over the Amazon Basin, *J. Clim.*, *11*, 2898–2909.
- Manabe, S. (1969), Climate and the ocean circulation, 1. The atmospheric circulation and the hydrology of the Earth's surface, *Mon. Weather Rev.*, *97*, 739–774.
- Margulis, S. A., D. McLaughlin, D. Entekhabi, and S. Dunne (2002), Land data assimilation and estimation of soil moisture using measurements from the Southern Great Plains 1997 Field Experiment, *Water Resour. Res.*, *38*(12), 1299, doi:10.1029/2001WR001114.
- Mesinger, F. (1996), Improvements in quantitative precipitation forecasts with the Eta regional model at the National Centers for Environmental Prediction: The 48 km upgrade, *Bull. Am. Meteorol. Soc.*, *77*, 2637–2650.
- Mesinger, F., T. L. Black, and Z. I. Janjic (1988), A summary of the NMC step mountain (Eta) coordinate model, paper presented at Workshop on Limited-Area Modeling Intercomparison, Natl. Cent. for Atmos. Res., Boulder, Colo.
- Mintz, Y., and Y. Serafini (1981), Global fields of soil moisture and land-surface evapotranspiration: Research review—1980/81, *NASA Tech. Memo.*, 83907, 178–180.
- Mintz, Y., and Y. V. Serafini (1989), Global monthly climatology of soil moisture and water balance, *LMD Internal Rep.* 148, 102 pp., Lab. de Météorol. Dyn., Paris.
- Mintz, Y., and Y. V. Serafini (1992), A global monthly climatology of soil moisture and water balance, *Clim. Dyn.*, *8*, 13–27.
- Mintz, Y., and G. K. Walker (1993), Global fields of soil moisture and land surface evapotranspiration derived from observed precipitation and surface air temperature, *J. Appl. Meteorol.*, *32*, 1305–1334.
- Mishra, S. K., V. B. Rao, and M. A. Gan (2001), Structure and evolution of the large-scale flow and an embedded upper-tropospheric cyclonic vortex over northeast Brazil, *Mon. Weather Rev.*, *129*, 1673–1688.
- Pielke, R. A. (2001), Further comments on “The differentiation between grid spacing and resolution and their application to numerical modeling,” *Bull. Am. Meteorol. Soc.*, *82*, 699–700.
- Reichle, R. H., and R. D. Koster (2003), Assessing the impact of horizontal error correlations in background fields on soil moisture estimation, *J. Hydrometeorol.*, *4*, 1229–1242.
- Reichle, R. H., J. P. Walker, R. D. Koster, and P. R. Houser (2002), Extended vs. ensemble Kalman filtering for land data assimilation, *J. Hydrometeorol.*, *3*, 728–740.
- Robock, A., C. A. Schlosser, K. Y. Vinnikov, N. A. Speranskaya, and J. K. Entin (1998), Evaluation of AMIP soil moisture simulations, *Global Planet. Change*, *19*, 181–208.
- Rodell, M., et al. (2004), The Global Land Data Assimilation System, *Bull. Am. Meteorol. Soc.*, *85*, 381–394.
- Satyamurty, P., C. A. Nobre, and P. L. Silva Dias (1998), South America, in *Meteorology of the Southern Hemisphere*, *Meteorol. Monogr.*, vol. 49, pp. 119–139, Am. Meteorol. Soc., Boston, Mass.
- Sellers, P. J., Y. Mintz, Y. C. Sud, and A. Dalcher (1986), A simple biosphere model (SiB) for use within general circulation models, *J. Atmos. Sci.*, *43*, 505–531.
- Seluchi, M. E., F. A. Norte, P. Satyamurty, and S. C. Sin (2003), Analysis of three situations of the Foehn effect over the Andes (Zonda wind) using the Eta-CPTC regional model, *Weather Forecast.*, *18*, 481–501.
- Seuffert, G., H. Wilker, P. Viterbo, J.-F. Mahfouf, M. Drusch, and J.-C. Calvet (2003), Soil moisture analysis combining screen-level parameters and microwave brightness temperature: A test with field data, *Geophys. Res. Lett.*, *30*(10), 1498, doi:10.1029/2003GL017128.
- Shukla, J., and Y. Mintz (1982), Influence of land surface evapotranspiration on the Earth's climate, *Science*, *215*, 1498–1501.
- Silva Dias, P. L., W. H. Schubert, and M. DeMaria (1983), Large-scale response of the tropical atmosphere to transient forcing, *J. Atmos. Sci.*, *40*, 2689–2707.
- Sun, S., and Y. Xue (2001), Implementing a new snow scheme in Simplified Simple Biosphere Model (SSiB), *Adv. Atmos. Sci.*, *18*, 335–354.
- Tanajura, C. A. S. (1996), Modeling and analysis of the South American summer climate, Ph.D. thesis, 164 pp., Univ. of Md., College Park.
- Tanajura, C. A. S., and J. Shukla (2000), Modeling the effects of the Andes on the South American summer climate, *Tech. Rep.* 83, 44 pp., Cent. for Ocean-Land-Atmos. Stud., College Park, Md.
- Thornthwaite, C. W. (1948), An approach toward a rational classification of climate, *Geogr. Rev.*, *38*, 55–94.
- Virji, H. (1981), A preliminary-study of summertime tropospheric circulation patterns over South America estimated from cloud winds, *Mon. Weather Rev.*, *109*, 599–610.
- Willmott, C. J., C. M. Rowe, and Y. Mintz (1985), Climatology of the terrestrial seasonal water cycle, *J. Clim.*, *5*, 589–606.
- Xue, Y., P. J. Sellers, J. Kinter, and J. Shukla (1991), A simplified biosphere model for global climates studies, *J. Clim.*, *4*, 354–364.
- Xue, Y., F. J. Zeng, K. Mitchell, Z. Janjic, and E. Rogers (2001), The impact of land surface processes on the simulation of the U.S. hydrological cycle: A case study of 1993 US flood using the Eta/SSiB regional model, *Mon. Weather Rev.*, *129*, 2833–2860.
- Xue, Y., S. Sun, D. Kahan, and Y. Jiao (2003), The impact of parameterizations in snow physics and interface processes on the simulation of snow cover and runoff at several cold region sites, *J. Geophys. Res.*, *108*(D22), 8859, doi:10.1029/2002JD003174.
- Walker, J. P., and P. R. Houser (2001), A methodology for initializing soil moisture in a global climate model: Assimilation of near-surface soil moisture observations, *J. Geophys. Res.*, *106*, 11,761–11,774.
- Weaver, C. P., and R. Avissar (2001), Atmospheric disturbances caused by human modification of the landscape, *Bull. Am. Meteorol. Soc.*, *82*, 269–281.
- Weisse, R., H. Heyen, and H. von Storch (2000), Sensitivity of a regional atmospheric model to a sea state-dependent roughness and the need for ensemble calculations, *Mon. Weather Rev.*, *128*, 3631–3642.
- Zhang, H., and C. S. Frederiksen (2003), Local and nonlocal impacts of soil moisture initialization on AGCM seasonal forecasts: A model sensitivity study, *J. Clim.*, *16*, 2117–2137.

S. C. Chou and J. Marengo, Centro de Previsão do Tempo e Estudos Climáticos, Instituto Nacional de Pesquisas Espaciais, Cachoeira Paulista, 12630-000 Sao Paulo, Brazil.

L. G. G. de Goncalves, M. Rodell, and D. L. Toll, Hydrological Sciences Branch, Code 614.3, NASA Goddard Space Flight Center, Greenbelt, MD 20771, USA. (gustavo@hsb.gsfc.nasa.gov)

P. R. Houser, Center for Research on Environment and Water, George Mason University, 4041 Powder Mill Road, Suite 302, Calverton, MD 20705-3106, USA.

W. J. Shuttleworth, Department of Hydrology and Water Resources, University of Arizona, Tucson, AZ 85721, USA.

Y. Xue, Department of Geography, 1255 Bunche Hall, University of California, Box 951524, Los Angeles, CA 90095-1524, USA.